British Journal of Pharmacology (2002) 136, 330–338
www.nature.com/bjp

Effects of thymol on calcium and potassium currents in canine and human ventricular cardiomyocytes

[1]János Magyar, [1]Norbert Szentandrássy, [1]Tamás Bányász, [1]László Fülöp, [2]András Varró & *,[1]Péter P. Nánási

[1]Department of Physiology, University Medical School of Debrecen, H-4012 Debrecen, P.O. Box 22, Hungary and [2]Department of Pharmacology and Pharmacotherapy, University of Szeged, H-6701 Szeged, P.O. Box 427, Hungary

1 Concentration-dependent effects of thymol (1–1000 μM) was studied on action potential configuration and ionic currents in isolated canine ventricular cardiomyocytes using conventional microelectrode and patch clamp techniques.

2 Low concentration of thymol (10 μM) removed the notch of the action potential, whereas high concentrations (100 μM or higher) caused an additional shortening of action potential duration accompanied by progressive depression of plateau and reduction of V_{max}.

3 In the canine cells L-type Ca current (I_{Ca}) was decreased by thymol in a concentration-dependent manner (EC_{50}: 158±7 μM, Hill coeff.: 2.96±0.43). In addition, thymol (50–250 μM) accelerated the inactivation of I_{Ca}, increased the time constant of recovery from inactivation, shifted the steady-state inactivation curve of I_{Ca} leftwards, but voltage dependence of activation remained unaltered. Qualitatively similar results were obtained with thymol in ventricular myocytes isolated from healthy human hearts.

4 Thymol displayed concentration-dependent suppressive effects on potassium currents: the transient outward current, I_{to} (EC_{50}: 60.6±11.4 μM, Hill coeff.: 1.03±0.11), the rapid component of the delayed rectifier, I_{Kr} (EC_{50}: 63.4±6.1 μM, Hill coeff.: 1.29±0.15), and the slow component of the delayed rectifier, I_{Ks} (EC_{50}: 202±11 μM, Hill coeff.: 0.72±0.14), however, K channel kinetics were not much altered by thymol. These effects on Ca and K currents developed rapidly (within 0.5 min) and were readily reversible.

5 In conclusion, thymol suppressed cardiac ionic channels in a concentration-dependent manner, however, both drug-sensitivities as well as the mechanism of action seems to be different when blocking calcium and potassium channels.

British Journal of Pharmacology (2002) **136,** 330–338

Keywords: Cardiac myocytes; electrophysiology; potassium currents; calcium current; thymol; anaesthesia; human myocytes

Abbreviations: APD, action potential duration; G_{Ca}, Ca conductance; I_{Ca}, Ca current; I_{Kr}, rapid component of the delayed rectifier K current; I_{Ks}, slow component of the delayed rectifier K current; I_{K1}, inward rectifier K current; I_{to}, I_{K1}, transient outward K current; V_m, membrane potential; V_{max}, maximum rate of depolarization of action potential

Introduction

Thymol (2-isopropyl-5-methylphenol) is widely used as a general antiseptic in the medical practice, agriculture, cosmetics and food industry (Aeschbach *et al*., 1994; Lee *et al*., 1997; Manou *et al*., 1998). Due to its potent fungicide, bactericide and antioxidant properties thymol is applied primarily in dentistry for treatment of oral infections (Twetman *et al*., 1995; Shapiro & Guggenheim, 1995; Ogaard *et al*., 1997). Thymol was also shown to have strong antiinflammatory action by decreasing the release of inflammatory metabolites like prostanoids, interleukins, and leukotrienes (Skold *et al*., 1998; Yucel-Lindberg *et al*., 1999). Thymol is added as a stabilizer to several therapeutic agents, including halothane, and the drug was shown to accumulate in the vaporizer during anaesthesia. In spite of the widespread application of thymol in medical practice, little is known about its effects in mammalian cardiac tissues. Therefore, the aim of the present work was to study the effects of thymol on action potential configuration and transmembrane ionic currents in isolated canine and healthy human ventricular cardiomyocytes.

*Author for correspondence; E-mail: nanasi@phys.dote.hu

Methods

Cell isolation

Isolated canine ventricular myocytes were obtained from hearts of adult mongrel dogs using the segment perfusion technique (Magyar *et al*., 2000a). Briefly, the animals (10–20 kg) were anaesthetized with intravenous injection of 10 mg kg^{-1} ketamine hydrochloride (Calypsolvet) + 1 mg kg^{-1} xylazine hydrochloride (Rometar). The hearts were rapidly removed from the chest and one of the coronary

arteries (usually LAD) was cannulated and perfused with calcium-free JMM solution (Minimum Essential Medium Eagle Joklik Modification for Suspension Culture, Type M-0518, Sigma) for 5 min in order to remove calcium from the tissues. The pH of this solution was adjusted to 7.2 using $NaHCO_3$ when gassed with carbogen at 37°C. Dispersion of the cells was performed during a 30 min perfusion with JMM solution containing 20 μM $CaCl_2$ and 1 g l^{-1} collagenase (Worthington, Type CLS1). The enzyme was removed from the tissues during a 5 min additional perfusion with enzyme-free JMM solution. Dispersed ventricular cells were suspended in the same solution, filtered, sedimented and then transferred to MEM solution (Minimum Essential Medium Eagle, M-0643, Sigma) containing 2.5 mM $CaCl_2$ and having pH adjusted to 7.35. This cell isolation procedure yielded a miscellaneous mixture of epicardial, endocardial and mid-myocardial cells. The myocytes were rod shaped and showed clear striation when the external calcium was restored following cell isolation. Cells were stored in MEM solution overnight at 15°C.

Human ventricular cells were prepared from hearts of general organ donor patients undergoing aortic valve transplantation surgery. The procedures used on human tissues have been approved by a local ethical committee and comply with the current laws of Hungary. The myocytes were isolated using a recently developed enzymatic dissociation procedure (Magyar *et al*., 2000b). After explantation and removal of the valves, hearts were transported into the laboratory in cold cardioplegic solution. A portion of the left ventricular wall was excised together with its arterial branch and was mounted on a modified Langendorff apparatus, where it was perfused through the left anterior descending coronary artery according to the following sequence: (1) Modified Tyrode solution (containing: NaCl, 135; KCl, 4.7; KH_2PO_4, 1.2; $MgSO_4$, 1.2; HEPES, 10; $NaHCO_3$, 4.4; glucose 10 mM; pH = 7.2) for 10 min; (2) Ca^{2+}-free modified Tyrode for 10 min; (3) Ca^{2+}-free modified Tyrode containing collagenase (660 mg l^{-1}, type I, Sigma), elastase (45 mg l^{-1}, type III, Sigma), taurine (50 mM) and bovine albumine (2 g l^{-1}, fraction V, fatty acid free, Sigma) for 45 min; and (4) After this step of enzymatic digestion the solution was supplemented with protease (120 mg l^{-1}, type XIV, Sigma) for a further 40–60 min. Portion of the left ventricular wall, that was clearly digested by the enzymes, were cut into small pieces and either stored in KB-medium (Isenberg & Klöckner, 1982), or equilibrated for 15 min in modified Tyrode containing 1.25 mM $CaCl_2$ and 50 mM taurine. Single myocytes were obtained from the tissue chunks after gentle agitation. During the entire isolation procedure the solutions were oxygenated (100% O_2) and the temperature was maintained at 37°C. The cells were allowed to sediment for 10 min, then the supernatant was decanted and replaced by fresh solution. This procedure was repeated for three times. The cells in KB-medium were stored at 4°C, while those stored in modified Tyrode solution were maintained at 12–14°C before use.

Action potential recording

Action potentials were recorded from Ca^{2+}-tolerant canine ventricular cells superfused with oxygenated Tyrode solution at 37°C. The bathing medium contained NaCl 140, KCl 5.4, $CaCl_2$ 2.5, $MgCl_2$ 1.2, Na_2HPO_4 0.35, HEPES 5, glucose 10 mM, at pH 7.4. Transmembrane potentials were recorded using glass microelectrodes filled with 3 M KCl and having tip resistance between 20 and 40 MΩ. These electrodes were connected to the input of an Axoclamp-2B amplifier (Axon Instruments). The cells were continuously paced through the recording electrode at a steady cycle length of 1000 ms using 1 ms wide rectangular current pulses with 120% threshold amplitude. Action potentials were digitized at 100 kHz using Digidata 1200 A/D card (Axon Instruments) and stored for later analysis.

Voltage clamp

Transmembrane currents were recorded in oxygenated Tyrode solution at 37°C. Suction pipettes, fabricated from borosilicate glass, had tip resistance of 2 MΩ after filling with pipette solution composed of KCl 110, KOH 40, HEPES 5, EGTA 10, TEACl 20, K-ATP 3 and GTP 0.25 mM, or alternatively, K-aspartate 100, KCl 45, $MgCl_2$ 1, EGTA 10, HEPES 5, K-ATP 3 mM, when measuring Ca or K currents, respectively. The pH of these solutions were adjusted to 7.2 with KOH. I_{Ca} was blocked by 5 μM nifedipine, and 3 mM 4-

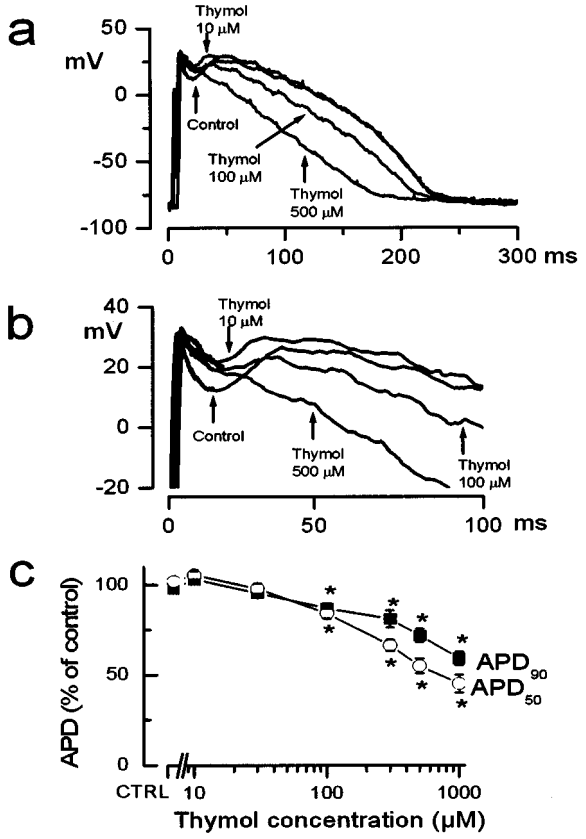

Figure 1 Effect of thymol on action potential configuration in canine ventricular myocytes. (a) Superimposed action potentials recorded before and in the presence of 10, 100 and 500 μM thymol. (b) Same action potentials shown in an extended scale to demonstrate the changes of the notch. (c) Cumulative concentration-dependent effects of thymol on action potential duration, measured at 50 and 90% levels of repolarization (APD_{50} and APD_{90}, respectively). Symbols and bars represent mean ± s.e.mean values, $n = 6$, asterisks denote significant ($P < 0.05$) changes from control values (CTRL).

aminopyridine was used to suppress I_{to} (both drugs were applied externally).

Currents were recorded with an Axopatch-200B amplifier (Axon Instruments) using the whole cell configuration of the patch clamp technique (Hamill *et al*., 1981). After establishing high (1–10 GΩ) resistance seal by gentle suction, the cell membrane beneath the tip of the electrode was disrupted by further suction or by applying 1.5 V electrical pulses for 1–5 ms. After this step, the intracellular solution was allowed to equilibrate with the pipette solution for a period of 5–10 min before starting the measurement. Ionic currents were normalized to cell capacitance, determined in each cell using short (25 ms) hyperpolarizing pulses from 0 mV to −10 mV. The mean value for cell capacitance was 142±5.4 pF in canine and 116±13 pF in human myocytes. The series resistance was typically 4–8 MΩ before compensation (usually 50–80%). Experiments were discarded when the series resistance was high or substantially increasing during the measurement. Outputs from the clamp amplifier were digitized at 20 kHz using an A/D converter (Digidata-1200, Axon Instruments) under software control (pClamp 6.0, Axon Instruments). The applied experimental protocols are described in the results section where appropriate.

Myocytes were superfused with thymol for 3–4 min and washout lasted for 5 min. In experiments studying cumulative concentration-dependent effects, each concentration of thymol was applied for 1 min. All values presented are arithmetic means±s.e.mean. Student's *t*-test for paired data was applied following ANOVA to determine statistical significance. Differences were considered significant when the *P* value was less than 0.05.

The entire investigation conforms with the *Guide for the Care and Use of Laboratory Animals* published by the US National Institutes of Health (NIH publication No. 85-23, revised 1996) and with the principles outlined in the Declaration of Helsinki.

Results

Effect of thymol on action potential configuration in canine myocytes

Thymol induced cumulative concentration-dependent changes in action potential configuration (Figure 1a,b). At a low concentration of 10 μM, the only observed effect was a reduction in phase 1 repolarization and partial attenuation of the notch. Higher concentrations of thymol (100 μM and above) decreased also action potential duration and caused depression of the plateau potential. The shortening of APD was more pronounced at 50% than at 90% level of repolarization (Figure 1c). Moderate reductions in the maximum rate of depolarization (to 93.4±4.7%, 89.1±4.4% and 70.3±8.2% of the control) were observed

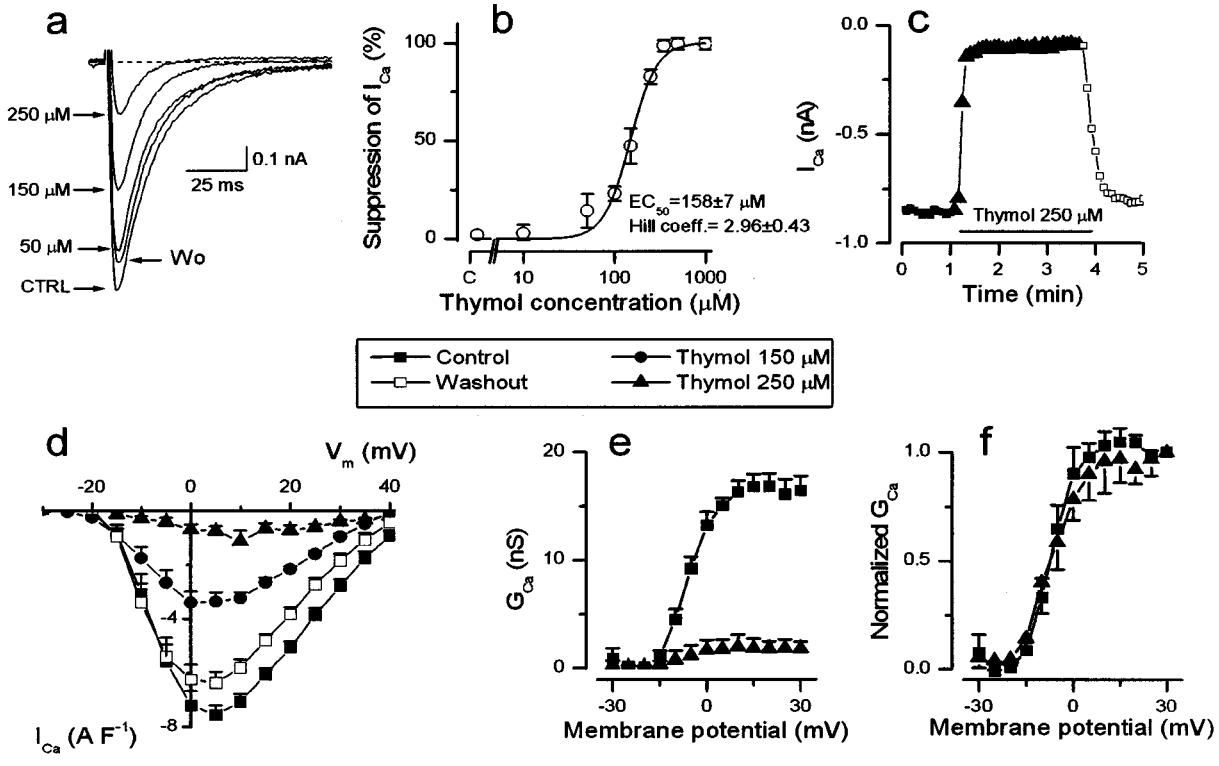

Figure 2 Effect of thymol on the amplitude of the Ca current in canine ventricular cells. (a) Superimposed I_{Ca} records, obtained before, during and after cumulative superfusion with 50, 150 and 250 μM thymol. (b) Cumulative concentration-dependent effects of thymol on peak I_{Ca} measured at +5 mV in four cells. The solid line was obtained by fitting data to the Hill equation. (c) Representative experiment showing the time scale of development and reversion of the drug-induced changes in I_{Ca}. (d) Current-voltage relationship obtained for peak I_{Ca} in seven cells in control, in the presence of 150 and 250 μM thymol, and following washout of the drug. (e) Voltage dependence of activation of calcium conductance (G_{Ca}) in control and in the presence of 250 μM thymol. (e) G_{Ca}-V_m relationships obtained from the experiment shown in (f), but G_{Ca} values were normalized to G_{Ca} obtained at +30 mV, and the results were fitted to a two-state Boltzmann model (solid curves).

in the presence of 300, 500 and 1000 μM thymol, respectively ($P<0.05$, $n=6$), indicating that these higher concentrations block fast sodium channels. No change in the resting potential was observed even at the highest concentration studied (-78.4 ± 2.2 mV versus -78.3 ± 6.2 mV at 1000 μM).

Effect of thymol on L-type calcium current in canine myocytes

Peak I_{Ca} was measured at a rate of 0.2 Hz using depolarizing voltage pulses of 400 ms duration clamped from the holding potential of -40 mV to the test potential of $+5$ mV. K currents were blocked by the externally applied 4-aminopyridine and internally applied TEACl. Stability of I_{Ca} was monitored at least for 5 min before cumulative application of thymol (from 1 to 1000 μM, each concentration for 1 min). Thymol displayed a concentration-dependent suppressive effect on peak I_{Ca} (Figure 2a). Inhibition of the current was statistically significant from the concentration of 50 μM (inhibition of $14.3\pm8.65\%$, $P<0.05$, $n=4$) and above. Fitting results to the Hill equation yielded an EC_{50} of 158 ± 7 μM and a slope factor of 2.96 ± 0.43 (Figure 2b). The effect of thymol on peak I_{Ca} developed rapidly (within 30 s) and was fully reversible (Figure 2c).

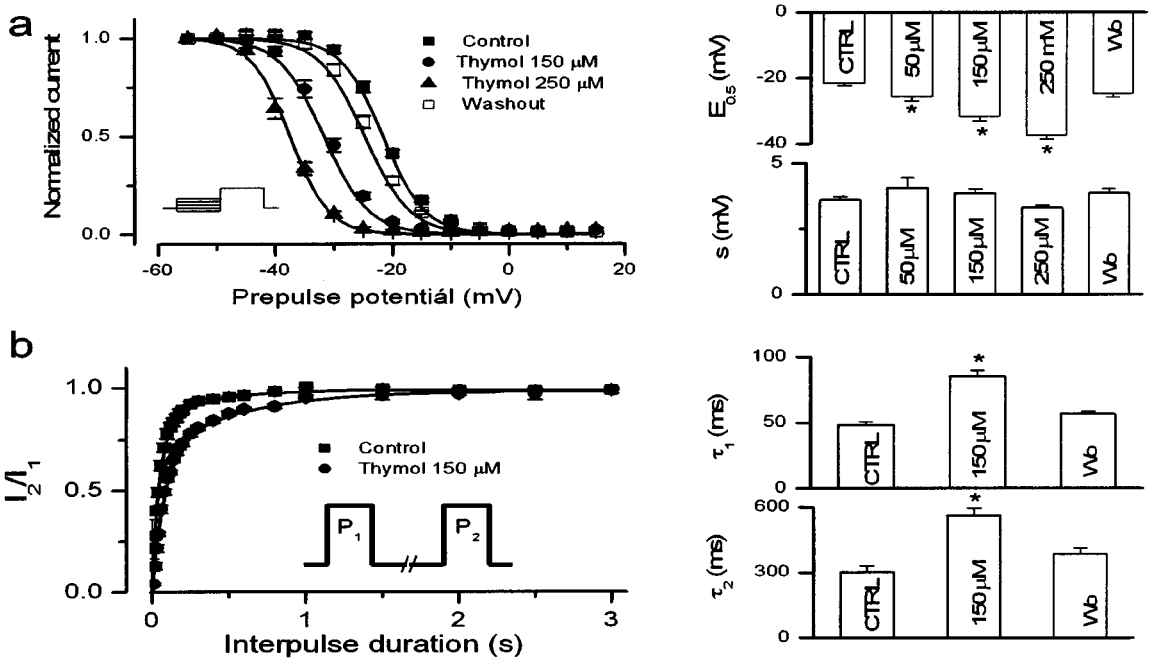

Figure 3 Effect of thymol on steady-state inactivation and recovery from inactivation of the Ca current in canine ventricular cells. (a) Voltage-dependence of steady-state inactivation of I_{Ca} determined using paired-pulse protocol in the presence and absence of thymol in five cells. Solid curves were obtained by fitting data to a two-state Boltzmann model. Estimated midpoint potentials ($E_{0.5}$) and slope factors (s) are presented in the right panel. (b) Time course of recovery from inactivation measured in control and in the presence of 150 μM thymol in five cells using twin-pulse protocol. The estimated fast and slow time constants are shown in the right panel.

Table 1 Effect of thymol on inactivation kinetics of calcium current in canine and human myocytes

(a) Canine myocytes ($n=7$)

	τ_1 (ms)	A_1 (A F^{-1})	τ_2 (ms)	A_2 (A F^{-1})
Control	12.1 ± 0.3	-8.4 ± 0.2	82.0 ± 1.9	-1.33 ± 0.07
Thymol 50 µM	12.0 ± 0.6	-6.4 ± 0.2*	81.8 ± 4.1	-0.53 ± 0.09*
Thymol 150 µM	8.6 ± 0.7*	-3.9 ± 0.1*	–	–
Thymol 250 µM	6.2 ± 0.1*	-3.0 ± 0.1*	–	–
Washout	11.7 ± 0.4	-7.5 ± 0.2*	92.9 ± 4.1	-0.92 ± 0.07*

(b) Human myocytes ($n=4$)

	τ_1 (ms)	A_1 (A F^{-1})	τ_2 (ms)	A_2 (A F^{-1})
Control	13.1 ± 1.3	-8.9 ± 0.7	83.1 ± 12	-1.19 ± 0.2
Thymol 250 µM	8.1 ± 1.1*	-2.8 ± 0.7*	42.5 ± 5*	-0.02 ± 0.01*
Washout	12.9 ± 1.5	-7.6 ± 0.5	9.6 ± 23	-7.0 ± 0.27

The decay of I_{Ca} was fitted as a sum of two exponential components, each characterized with a time constant (τ) and relative amplitude (A). Index numbers 1 and 2 refer to the fast and slow components, respectively. Mean$\pm$s.e.mean are given, asterisks denote significant ($P<0.05$) changes from control values.

Current-voltage relations for I_{Ca} were obtained by applying a series of test pulses increasing up to +40 mV in 5 mV steps in absence and presence of the thymol, and peak values of I_{Ca} were plotted against their respective test potentials. No shift in the current-voltage relationship was observed in seven myocytes after application of 150 and 250 μM thymol (Figure 2d). Calcium conductance (G_{Ca}) was calculated at each membrane potential by dividing the peak current by its driving force (the difference between the applied test potential and the reversal potential for I_{Ca}, estimated to be +55 mV). As shown in Figure 2e, the Ca-conductance was significantly diminished by 250 μM thymol at each membrane potential studied, however, when G_{Ca} values of both curves were normalized to the respective G_{Ca} obtained at +30 mV, the G_{Ca}-V_m relationships were almost identical (Figure 2f). This latter result suggests that voltage dependence of activation of I_{Ca} is not affected by thymol.

In contrast to the unchanged voltage dependence of activation, inactivation kinetics were seriously altered in the presence of thymol in a reversible manner. In order to study the voltage-dependence of steady-state inactivation of I_{Ca} test depolarizations to +5 mV were preceded by a set of prepulses clamped to various voltages between −55 and +20 mV for 500 ms. Peak currents measured after these prepulses were normalized to the peak current measured after the −55 mV prepulse and plotted against the respective prepulse potential. The data were fitted to the two-state Boltzmann function (Figure 3a). Superfusion of the cells with 50, 150 and 250 μM thymol shifted the midpoint potentials by 5.1±1, 10.4±1.2 and 17.4±1.6 mV, respectively, ($P<0.05$, $n=5$) from the control value of −21.6±0.7 mV towards more negative potentials without significant changes in the slope factor.

In addition to increased steady-state inactivation, thymol also accelerated the time-dependent decay of I_{Ca}. This can be well detected on the analogue records shown in Figure 2a. The decay of I_{Ca} followed biexponential kinetics at +5 mV, characterized as a sum of a fast and a slow component in control. Application of increasing concentrations of thymol significantly reduced the relative amplitude of both components and decreased the time constant of the fast component. The slow component of inactivation was more sensitive to thymol than the fast component, since it was completely blocked by higher thymol concentrations (150 and 250 μM) in all of the seven experiments performed, allowing only monoexponential fitting of these curves (Table 1a).

Time course of recovery from inactivation was studied using a twin-pulse protocol. Two 400 ms long depolarizations to +5 mV were separated by an interpulse interval having variable duration. Peak I_{Ca} amplitude measured by the second pulse was normalized to that measured by the first pulse and their ratio (I_2/I_1) was plotted as a function of the interpulse interval. These curves were fitted as a sum of two exponential components. Both the fast and slow time constants of recovery from inactivation were increased significantly by 150 μM thymol in a reversible manner (from 47.2±2.7 to 83±4.8 ms and from 292±33 to 569±41 ms, respectively, $P<0.05$, $n=5$; Figure 3b).

Effect of thymol on calcium current in undiseased human ventricular cells

Effects of thymol (250 μM) in the human cells ($n=4$) were qualitatively similar to those obtained in canine myocytes (Figure 4). Thymol suppressed the peak value of I_{Ca} at each

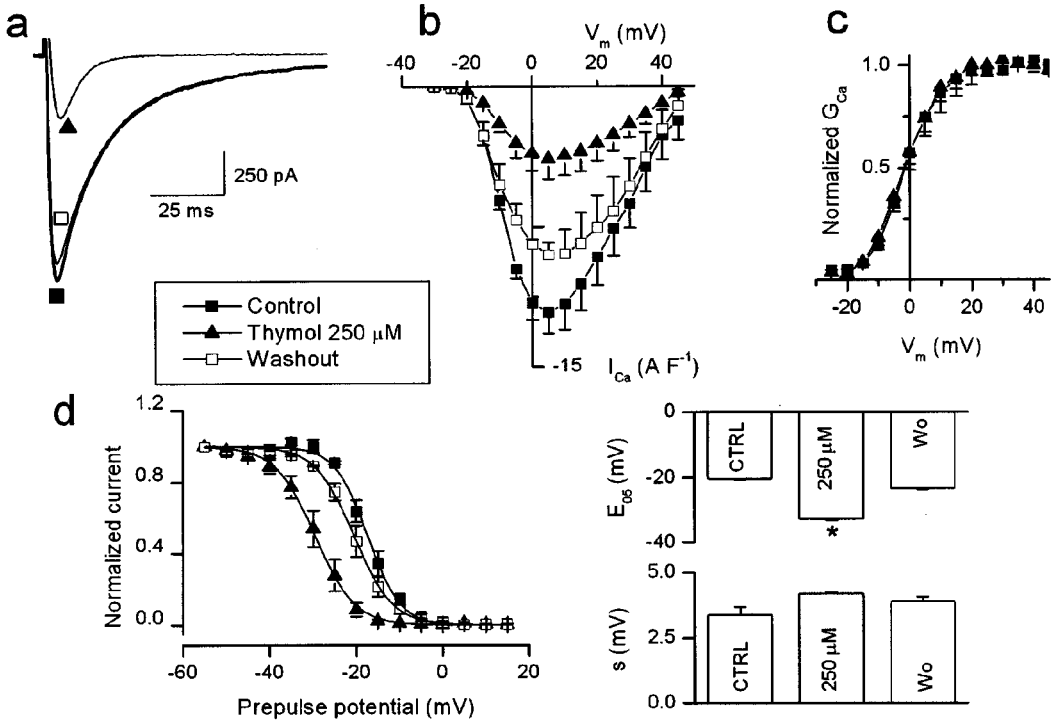

Figure 4 Effect of 250 μM thymol on the Ca current in ventricular myocytes ($n=4$) isolated from undiseased human hearts. (a) Superimposed I_{Ca} records measured at +5 mV. (b) Current-voltage relationships. (c) Normalized G_{Ca}-V_m relationships. (d) Voltage dependence of steady-state inactivation. Measurements were performed as described for canine cells in the legend of Figures 2 and 3.

test potential studied (from -12.1 ± 1.1 to -3.8 ± 1.1 A F-1 at $+5$ mV, $P<0.05$) without changing the shape of the I–V relationship and the normalized G_{Ca}-V_m curve. Effect on the voltage-dependence of steady-state inactivation was also similar to those seen in the canine cells: the midpoint of the Boltzmann function was shifted from -20.3 ± 0.52 mV to -32.7 ± 0.17 mV (12.4 ± 0.7 mV leftward shift, $P<0.05$), while the slope factor remained unaltered. Similar to results obtained in canine cells, 250 μM thymol reduced the amplitude of both components and decreased the respective time constants (Table 1b). Since the suppressive effect of thymol was weaker in human cells than in canine myocytes, the slow component was not fully abolished, only markedly reduced. These single-dose effects, requiring not more than 1 min superfusion with thymol, were readily reversible. However, when longer thymol exposures were applied (e.g. when measuring the I–V relationship) the reversion was only partial in human myocytes.

Effect of thymol on the transient outward potassium current in canine myocytes

The transient outward current, I_{to}, was studied using voltage pulses of 400 ms duration clamped from the holding potential of -80 mV to test potentials ranging between -10 and $+60$ mV. Each of these test pulses were preceded by a 5 ms long prepulse to -40 mV in order to inactivate the Na current. I_{to} was decreased by thymol in a concentration-dependent manner (Figure 5a,b). This effect developed at relatively low concentrations (suppression of $5.2\pm2.4\%$ and $17.4\pm2.7\%$ were observed in the presence of 1 and 10 μM thymol, respectively, $P<0.05$, $n=4$) in sharp contrast to results obtained previously with I_{Ca}. The Hill equation, used to describe the concentration-dependency of the thymol-effect, yielded an EC_{50} of 60.6 ± 11.4 μM for I_{to}, a value significantly lower than obtained for I_{Ca} in canine myocytes (158 μM). The Hill coefficient was close to unity (1.03 ± 0.11) suggesting that one single binding site may be involved in the suppressive effect of thymol on I_{to}. The effect of 100 μM thymol on the amplitude of I_{to} developed within 30 s and was fully reversible within 1 min of washout (Figure 5c). The blocking effect of thymol on I_{to} was not voltage-dependent as indicated by the peak current-voltage relationships presented in Figure 5d. Similarly, no change in the voltage dependence of the steady-state inactivation of I_{to} was observed (midpoint potentials of -38.4 ± 3 mV and -39.3 ± 3.6 mV were determined in the absence and presence of 100 μM thymol, respectively, N.S., $n=6$, Figure 5e). The decay of I_{to} was best fitted as a sum of two exponential components in canine cells, described by a fast (2.3 ± 0.3 ms) and a slow (10.4 ± 1.3 ms) time constant at $+50$ mV in control. Application of 100 μM thymol had no significant effect on the fast time constant

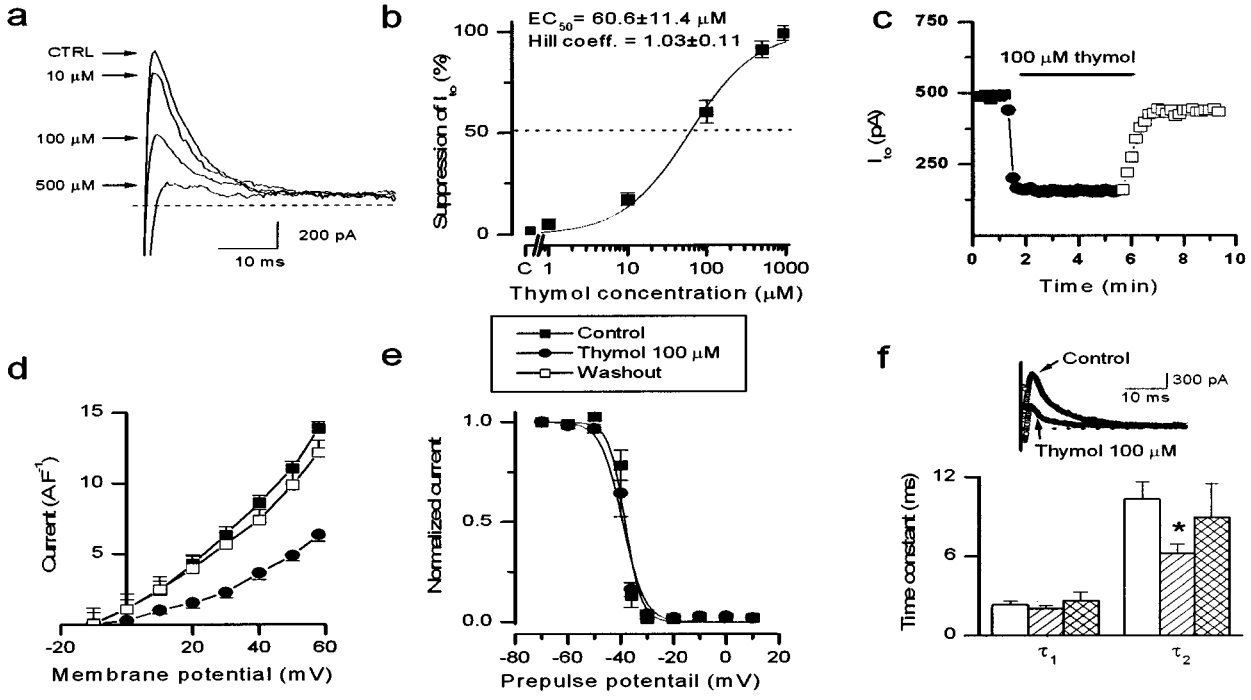

Figure 5 Effect of thymol on the transient outward current in canine myocytes. (a) Superimposed records of I_{to} measured at $+50$ mV in control and in the presence of 10, 100 and 500 μM thymol. (b) Cumulative concentration-dependent effects of thymol on I_{to} measured at $+50$ mV in four cells. The solid line was obtained by fitting data to the Hill equation. (c) Representative experiment showing the time scale of development and reversion of the thymol-induced changes in I_{to}. (d) Effect of 100 μM thymol on I_{to} densities measured in eight myocytes as a function of the test potentials varied from -10 to $+60$ mV. (e) Effect of 100 μM thymol on the voltage-dependence of steady-state inactivation of I_{to} studied in six myocytes. Before testing peak I_{to} current amplitudes at $+50$ mV, depolarizing prepulses to various potentials, each having 500 ms duration, were applied. The peak current obtained after each prepulse was normalized to that arising from the holding potential of -80 mV. These ratios of currents were plotted against their prepulse potentials and fitted to a two-state Boltzmann model (solid lines). (f) Fast and slow time constants for inactivation of I_{to} obtained before (empty columns), during (striped columns) and after (crossed columns) superfusion with 100 μM thymol in eight cells. The original I_{to} records are presented in the inset.

(2.0±0.25 ms, N.S.) but decreased the slow time constant to 6.2±0.7 ms ($P<0.05$, $n=8$; Figure 5f).

Effect of thymol on the rapid and slow components of the delayed rectifier K current

In voltage clamped canine ventricular myocytes ($n=4$) thymol caused concentration-dependent block on the rapid component of the delayed rectifier, I_{Kr}. The current was activated using depolarizing voltage pulses of 150 ms duration clamped from the holding potential of −40 mV to the test potential of +10 mV. The decaying current tails recorded at −40 mV after the end of the test pulse was assessed as I_{Kr} (Figure 6a). These short depolarizations are suitable to activate a sufficient amount of I_{Kr} without substantial contamination with I_{Ks} (Varró *et al*., 2000). Tail current amplitudes were significantly decreased by thymol in a reversible and concentration-dependent manner (Figure 6a,b). Fitting these data to the Hill equation yielded EC_{50} value of 63.4±6.1 μM and a slope factor of 1.29±0.15. In another set of experiments, performed in five cells, I_{Kr} was activated at various voltages ranging from −30 to +30 mV for 150 ms. One hundred μM thymol failed to alter the voltage dependence of activation of the current although the inhibition was evident at all voltages positive to −20 mV. (Figure 6c).

The slow component of the delayed rectifier, I_{Ks} was activated using long (3000 ms) depolarizing pulses clamped to +50 mV, and the fully activated current, measured at the end of depolarization, was considered as a measure of I_{Ks} (Figure 6d). In the five myocytes studied thymol caused concentration-dependent and reversible block of I_{Ks} characterized by an EC_{50} value of 202±11 μM and a Hill coefficient of 0.72±0.14 (Figure 6e). Similar to results obtained on I_{Kr}, the thymol induced block of I_{Ks} was not voltage-dependent between +10 and +60 mV (Figure 6f).

Effect of thymol on the inward rectifier K current

The steady-state current-voltage characteristics of the membrane were studied using voltage clamp steps of 400 ms duration ranging between −125 and +65 mV and arising from the holding potential of −80 mV. The currents measured at the end of these potential steps were plotted against their respective test potentials – presented as steady-state I–V relationships. The slope of the negative branch of the I–V curve is determined by the density of the inward rectifier K current, I_{K1}. Thymol (100 μM) decreased the slope of the negative branch of the I–V curve indicating an inhibitory effect of the drug on I_{K1} (Figure 7a). At the test potential of −125 mV 100 μM thymol reduced I_{K1} density from the control value of −43.3±1.6 A F^{-1} to −34.9±1.6 A F^{-1} ($P<0.05$, $n=8$). Superimposed I_{K1} currents recorded at −125 mV before, in the presence, and after removal of 100 μM thymol is presented in Figure 7b. The blocking effect of thymol on I_{K1} developed rapidly and was readily reversible (Figure 7c), similar to results obtained on other ionic currents with thymol.

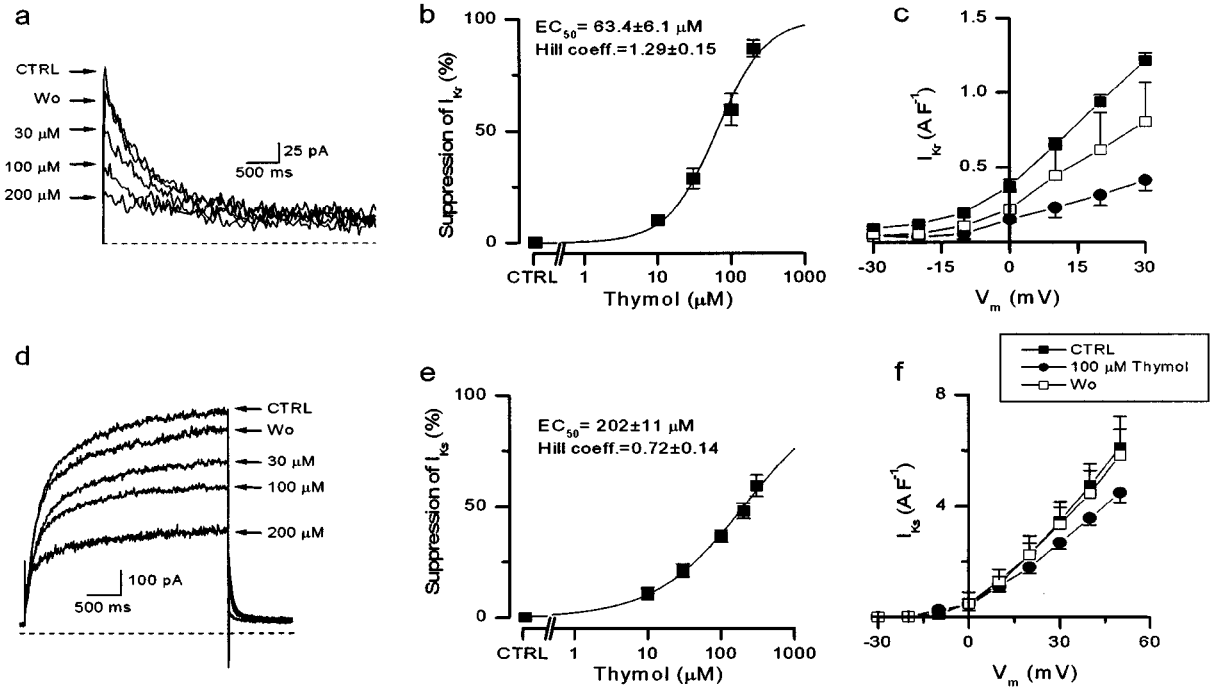

Figure 6 Concentration-dependent effects of thymol on the rapid (I_{Kr}, a–c) and slow (I_{Ks}, d–f) components of the delayed rectifier K current in canine cells. I_{Kr} was evaluated as a tail current appearing upon repolarization to −40 mV following a short (150 ms) depolarization to +10 mV. I_{Ks} was activated using a long (3000 ms) depolarization to +50 mV. (a, d) Superimposed records of I_{Kr} and I_{Ks}, respectively, before, in the presence of, and after removal of thymol. Dashed lines indicate zero current. (b, e) Concentration-response curves obtained with thymol for I_{Kr} ($n=4$) and I_{Ks} ($n=5$). EC_{50} values and Hill coefficients were determined using the Hill equation (solid lines). (c, f) Effect of 100 μM thymol on the voltage dependence of I_{Kr} and I_{Ks} (both $n=5$). Test potentials applied for activation of the currents (for 150 ms and 3000 ms, respectively) are given in the abscissa.

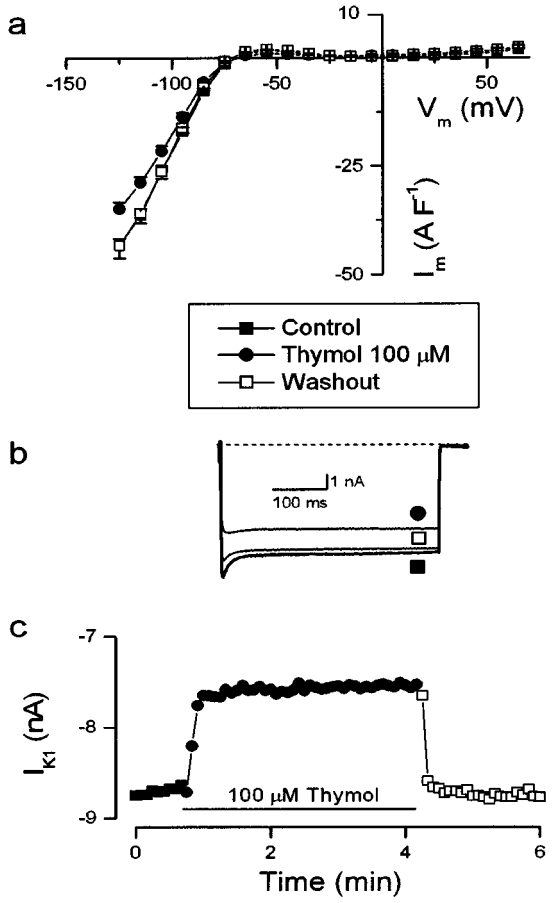

Figure 7 Effect of thymol on the inward rectifier K current in canine cells. (a) Steady-state current-voltage relationship of the membrane determined at the end of 400 ms long voltage steps clamped to membrane potentials showed in the abscissa ($n=8$). (b) Superimposed records of I_{K1} current traces measured at -125 mV in control, in the presence of, and after washing out of 100 μM thymol. (c) Representative experiment showing the time scale of development and reversibility of the effect of 100 μM thymol on I_{K1}, measured at -125 mV.

Discussion

In this study we have established that practically all cardiac ion currents examined were modified by thymol. This suppressive effect, however, was substantially different for K and Ca currents. The Hill coefficient estimated for the thymol-induced inhibition of K currents (I_{to}, I_{Kr} and I_{Ks}) were close to unity, suggesting the involvement of single, independent binding sites. Furthermore, except the acceleration of decay of I_{to}, no changes kinetic properties of these currents were observed in the presence of thymol. In contrast, suppressive effect of thymol on I_{Ca} was characterized by a Hill coefficient close to 3, suggesting positive cooperation between the binding sites involved, or alternatively, contribution of more than one mechanism in the block. Due to the hydrophobic character of the molecule thymol may approach channel proteins through the lipid phase of the membrane and may alter their local environment. This mechanism may likely be involved in the effect of thymol on ion channels in general, however, cannot account for the differences found between blockade of Ca and K channels, since all these channels (except I_{K1}) contain largely similarly arranged six transmembrane domain assembly (Shieh *et al*., 2000). It is possible, therefore, that in addition to postulated lipid interactions, thymol may bind to and thus modify the channel proteins as well. In our experiments marked leftwards shift in the voltage-dependence of steady-state inactivation of I_{Ca} was observed with thymol (Figures 3 and 4d), which may increase the voltage-dependent rate constant for inactivation resulting in acceleration of the time constant for inactivation as demonstrated in Table 1. Based on these results, the blocking effect of thymol on cardiac Ca current resembles that of the conventional Ca-entry blocker verapamil. Indeed, thymol was reported to effectively suppress Ca current in neuronal membranes (Gyri *et al*., 1991). Although relatively low concentrations of thymol were shown to induce Ca release from internal stores in neural (Kostyuk *et al*., 1991), smooth muscle (Hisayama & Takayanagi, 1986), skeletal muscle (Szentesi *et al*., 2001), and cardiac tissues (own unpublished results), this effect might not substantially modify the interpretation of present results on ion currents due to the presence of 10 mM EGTA in our pipette solution. This was not the case in action potential measurements, performed with conventional sharp microelectrodes containing EGTA-free KCl, therefore, the possible contribution of the thymol-induced Ca release to changes in action potential morphology cannot be ruled out in these experiments.

The effect of thymol on action potential configuration of canine myocytes can be well explained by the differences in EC_{50} values estimated for the suppressive effects of thymol on various ion currents. Low concentration (10 μM) abolished the notch of the action potential without further changes in the action potential morphology, whereas higher concentrations (100 μM and above) caused shortening of APD and depression of the plateau. The former effect is likely due to inhibition of I_{to}, and the latter due to blockade of I_{Ca}. This thymol-induced shortening of APD suggests that the effect of high thymol concentrations on APD is dominated by suppression of I_{Ca} in contrast to the inhibitory effect on I_{Kr} and I_{to}, in spite of the lower EC_{50} values obtained for K channel blockade.

It is important to emphasize that the effects of thymol on I_{Ca} were qualitatively similar in canine and healthy human ventricular cells, however, they were weaker in the latter. At a concentration of 250 μM thymol decreased peak I_{Ca} by 82.6%, the faster time constant for inactivation by 49.6%, and shifted the steady-state inactivation curve by -17.4 mV in canine myocytes. The respective values obtained in human cells were 68.6%, 38.2%, and -12.4 mV. In spite of these minor differences observed in canine and human myocytes, one may conclude that the mechanism of action of thymol on calcium channels is essentially similar in dog and human.

The multiple suppressive effect of thymol on cardiac ion currents (I_{Na}, I_{Ca}, I_{to}, I_{Kr}, I_{Ks} and I_{K1}), demonstrated in this study, may cause cardiac arrhythmias in case of incorporation of the appropriate amount of thymol. Since the compound is a commonly applied constituent of herbal complexes, mouth wash and dental medication, its accidental overdose or intentional intoxication (in case of suicide) can not be excluded. Probably it is more important from the therapeutic point of view that thymol is used to stabilize liquid halothane when applying for general anaesthesia.

Although the concentration of thymol is relatively low (0.01%) in the original halothane-thymol mixture, its concentration may dramatically increase due to accumulation of thymol in the vaporizer in case of improper use. In a perioperative cardiac arrest registry performed in pediatric patients two third of cases of cardiac arrest due to medication was considered to be a consequence of application of halothane (Morray *et al*., 2000). Indeed, halothane was shown to block I_{Ca} and I_K in guinea-pig ventricular myocytes with little effect on I_{K1} (Hirota *et al*., 1989). Similar results were obtained by Baum *et al*. (1994), where suppression of I_{Ca} was associated with a -11 mV leftward shift of the steady-state inactivation curve. Davies *et al*. (2000) found halothane to depress I_{to} in rat ventricular cells. These effects obtained with liquid halothane (containing also thymol) resembles our present results with thymol, raising the possibility that some of the cardiac effects ascribed previously to halothane may probably be attributed to the concomitant presence of thymol in the superfusate.

Financial support for the studies was obtained from grants to J. Magyar and P.P. Nánási and from the Hungarian Ministry of Health (ETT-52/2000, ETT-244/2000), the Hungarian Ministry of Education (FKFP-0243/2000) and Hungarian Research Fund (OTKA-T037334).

References

AESCHBACH, R., LOLIGER, J., SCOTT, B.C., MURCIA, A., BUTLER, J., HALLIWELL, B. & ARUOMA, O.I. (1994). Antioxidant actions of thymol, carvacrol, 6-gingerol, zingerone and hydroxytyrosol. *Food Chem. Toxicol.,* **32,** 31–36.

BAUM, V.C., WETZEL, G.T. & KLITZNER, T.S. (1994). Effects of halothane and ketamine on activation and inactivation of myocardial calcium current. *J. Cardiovasc. Pharmacol.,* **23,** 799–805.

DAVIES, L.A., HOPKINS, P.M., BOYETT, M.R. & HARRISON, S.M. (2000). Effects of halothane on the transient outward K^+ current in rat ventricular myocytes. *Br. J. Pharmacol.,* **131,** 223–230.

GYRI, J., KISS, T., SHCHERBATKO, A.D., BELAN, P.V., TEPIKIN, A.V., OSIPENKO, O.N. & SALÁNKI, J. (1991). Effect of Ag^+ on membrane permeability of perfused Helix pomatia neurons. *J. Physiol. (Lond.),* **442,** 1–13.

HAMILL, O.P., MARTY, A., NEHER, E., SAKMANN, B. & SIGWORTH, F.J. (1981). Improved patch-clamp techniques for high resolution current recording from cells and cell-free membrane patches. *Pflügers Arch.,* **391,** 85–100.

HIROTA, K., ITO, Y., MASUDA, A. & MOMOSE, Y. (1989). Effects of halothane on membrane ionic currents in guinea pig atrial and ventricular myocytes. *Acta Anaesth. Scand.,* **33,** 239–244.

HISAYAMA, T. & TAKAYANAGI, I. (1986). Some properties and mechanisms of thymol-induced release of calcium from the calcium store in guinea pig taenia coli. *Jpn. J. Pharmacol.,* **40,** 69–82.

ISENBERG, G. & KLÖCKNER, U. (1982). Isolated bovine ventricular myocytes. Characterization of action potential. *Pflügers Arch.,* **395,** 19–29.

KOSTYUK, P.G., BELAN, P.V. & TEPIKIN, A.V. (1991). Free calcium transients and oscillations in nerve cells. *Exp. Brain Res.,* **83,** 459–464.

LEE, S., TSAO, R., PETERSON, C. & COATS, J.R. (1997). Insecticidal activity of monoterpenoids to western corn rootworm (*Coleoptera: Chrysomelidae*) two-spotted spider mite (*Acari: Tetranychidae*), and house fly (*Diptera: Muscidae*). *J. Econ. Entomol.,* **90,** 883–892.

MAGYAR, J., BÁNYÁSZ, T., SZIGLIGETI, P., KÖRTVÉLY, Á., JENÁKOVITS, A. & NÁNÁSI, P.P. (2000a). Electrophysiological effects of bimoclomol in canine ventricular myocytes. *Naunyn-Schmiedberg's Arch. Pharmacol.,* **361,** 303–310.

MAGYAR, J., IOST, N., KÖRTVÉLY, Á., BÁNYÁSZ, T., VIRÁG, L., SZIGLIGETI, P., VARRÓ, A., OPINCARIU, M., SZÉCSI, J., PAPP, J.G. & NÁNÁSI, P.P. (2000b). Effects of endothelin-1 on calcium and potassium currents in undiseased human ventricular myocytes. *Pflügers Arch.,* **441,** 144–149.

MANOU, L., BOUILLARD, L., DEVLEESCHOUWER, M.J. & BAREL, A.O. (1998). Evaluation of the preservative properties of Thymus vulgaris essential oil in topically applied formulations under a challenge test. *J. Appl. Microbiol.,* **84,** 368–376.

MORRAY, J.P., GEIDUSCHEK, J.M., RAMAMOORTHY, C., HABER-KERN, C.M., HACKEL, A., CAPLAN, R.A., DOMINO, K.B., POSNER, K. & CHENEY, F.W. (2000). Anesthesia-related cardiac arrest in children: initial findings of the Pediatric Perioperative Cardiac Arrest (POCA) Registry. *Anesthesiology,* **93,** 6–14.

OGAARD, B., LARSSON, E., GLANS, R., HENRIKSSON, T. & BIRKHED, D. (1997). Antimicrobial effect of a chlorhexidine-thymol varnish (Cervitec) in orthodontic patients. A prospective, randomized clinical trial. *J. Orofac. Orthop.,* **58,** 206–213.

SHAPIRO, S. & GUGGENHEIM, B. (1995). The action of thymol on oral bacteria. *Oral Microbiol. Immunol.,* **10,** 241–246.

SHIEH, C.-C., COGHLAN, M., SULLIVAN, J.P. & GOPALAKRISHNAN, M. (2000). Potassium channels: molecular defects, diseases, and therapeutic opportunities. *Pharmacol. Rew.,* **52,** 557–593.

SKOLD, K., TWETMAN, S., HALLGREN, A., YUCEL-LINDBERG, T. & MODEER, T. (1998). Effect of a chlorhexidine/thymol-containing varnish on prostaglandin E_2 levels in gingival crevicular fluid. *Eur. J. Oral Sci.,* **106,** 571–575.

SZENTESI, P., COLLET, C., SÁRKÖZI, S., SZEGEDI, C., JONA, I., JACQUEMOND, V., KOVÁCS, L. & CSERNOCH, L. (2001). Effects of dantrolene on steps of excitation-contraction coupling in mammalian skeletal muscle fibres. *J. Gen. Physiol.,* **118,** 355–375.

TWETMAN, S., HALLGREN, A. & PETERSSON, L.G. (1995). Effect of antibacterial varnish on mutans streptococci in plaque form enamel adjacent to orthodontic appliances. *Caries Res.,* **29,** 188–191.

VARRÓ, A., BALÁTI, B., IOST, N., TAKÁCS, J., VIRÁG, L., LATHROP, D.A., LENGYEL, CS., TÁLOSI, L. & PAPP, J.GY. (2000). The role of the delayed rectifier component I_{Ks} in dog ventricular muscle and Purkinje fibre repolarization. *J. Physiol. (Lond.),* **523,** 67–81.

YUCEL-LINDBERG, T., TWETMAN, S., SKOLD-LARSSON, K. & MODEER, T. (1999). Effect of an antibacterial dental varnish on the levels of prostanoids, leukotriene B4, and interleukin-1 beta in gingival crevicular fluid. *Acta Odontol. Scand.,* **57,** 23–27.

(Received January 15, 2002
Revised March 12, 2002
Accepted March 13, 2002)